Compact Zeroth-order Resonance Loaded Microstrip Antenna with Enhanced Bandwidth for Wireless Body Area Networks/Brain Activity Detection

Kai Sun [1], Lin Peng [1,2,*], Quan Li [1], Xiaoming Li [1], and Xing Jiang [1]

[1] Guangxi Key Laboratory of Wireless Wideband Communication and Signal Processing
Guilin University of Electronic Technology, Guilin, Guangxi, 541004, China
[*]penglin528@hotmail.com, jiang_x@guet.edu.cn

[2] Guangxi Experiment Center of Information Science, Guilin, 541004, Guangxi, China
penglin528@hotmail.com

Abstract ― A novel bandwidth enhanced compact microstrip antenna for wireless body area networks (WBANs) applications is designed by loading zeroth-order resonator (ZOR) structure. The broadband was realized by combining the ZOR resonant frequency with the microstrip patch resonant frequency. The patch dimensions of the antenna are $0.212\lambda c \times 0.310\lambda c \times 0.027\lambda c$, where λc is the wavelength of the lower cutoff frequency. By using the ZOR, the bandwidth of the proposed antenna increased by 150% compared to the reference microstrip antenna. The proposed antenna was fabricated. The measured and simulated the -10 dB $|S_{11}|$ bandwidth are 5.5% (2.352-2.485 GHz) and 6.7% (2.320-2.481 GHz), respectively. Thus, the antenna covers the medical BAN (MBAN) band (2.36-2.4 GHz) and the 2.4–2.48 GHz Industrial, Scientific and Medical (ISM) band. From the simulated and measured results, both the microstrip patch mode and the ZOR mode of the proposed antenna radiate uni-directionally. The gains of the antenna are 2.56 dBi and 4.54 dBi at the ZOR mode and microstrip patch mode, respectively. The off-body characteristics of the antenna were investigated and compared with the free-space characteristics. As the antenna was mounted as off-body, the simulated and measured impedance bandwidths of the antenna are 5.5% (2.352-2.484 GHz) and 4.7% (2.35-2.465 GHz), respectively. Although the bandwidths are reduced, the ISM band and the MBAN band are still covered. Though the antenna with tissue backing has increased back radiation, good uni-directionally radiation patterns are also observed. The robust off-body performances reveal that the proposed antenna is a good candidate for WBAN applications. In addition, to evaluate its safety for brain activity detection, the electromagnetic radiation energy of antennas was considered and the safety performance of the antenna is studied by measuring the value of specific absorption rate (SAR).

Index Terms ― Band-width, brain activity detection, compact, off-body performance, SAR, wireless body-area network (WBAN), ZOR.

I. INTRODUCTION

In recent years, tremendous advancements have been developed in the field of body area network (BAN) electromagnetics, and revolutionary functionalities were achieved for the health monitoring, patient tracking, physiotherapy, wearable computing, battlefield survival, the Internet of Things (IoT), and so on. Thereby, BAN technology holds great promising for the revolutionizing of many aspects of the daily life of human beings [1-4], such as real-time online healthcare, patients can be tracked and monitored in normal or emergency conditions at their homes, hospital rooms, and in Intensive Care Units (ICUs). Typically, the type of communication within a WBAN can be classified into three modes, including on-body, in-body (or sometimes called through-body), and off-body communications [5]. Thus, the antennas applied on the WBAN require radiation pattern normal to the body surface and a smaller size. The frequency bands for BAN communication systems mainly include the 402–405 MHz Medical Implant Communication Services (MICS) band [5-6] that are primarily used for on-body and through-body communications, the 2.4–2.48 GHz Industrial, Scientific, and Medical (ISM) band [5, 7] as well as the 3.1–10.76 GHz Ultra-Wide Band (UWB) range [5, 8] that are primary used for off-body communication, and the medical BAN (MBAN) band that operates from 2.36 GHz to 2.4 GHz [5, 9]. As a vital component of WBAN, the antenna is very close to the human body, and it is required with the characteristics of lightweight, low profile and small size [3]. However, the performances of an antenna could be impaired by the loading effect of the loss of the tissue. Many antennas have been studied for WBAN applications, including monopole antennas [10], inverted-F antennas [11-12], microstrip patch antennas [13], artificial magnetic conducting surface

Submitted On: November 21, 2017
Accepted On: April 21, 2018

backed antennas [14] and so on. In [10], the vertical monopole antennas with narrow band and high-profile are studied for on-body communications. Reference [11] presents a broadband textile planar inverted-F antenna (PIFA), and [12] presents a dual-band Sierpinski fractal PIFA, and the antennas require complex 3-dimensional and thicker structures. Reference [13] utilizes microstrip patch antenna to statistical analyze the performance of on-body radio propagation, and the antenna is narrow bandwidth. In [14], a dual-band coplanar patch antenna integrated with an electromagnetic band gap substrate is described. The electromagnetic band-gap (EBG) substrate provides a high isolation between the antenna and human tissue, and the antenna covers the 2.45 GHz and 5.8 GHz wireless bands. However, the antenna still suffered from low front-to-back ratio (FBR). To obtain further compact antenna size, a novel zeroth-order resonance (ZOR) antenna with a spiral slotted ground plane was proposed in [15]. Though, the antenna in [15] is miniaturized, its bandwidth is very narrow. Moreover, multiband and broadband antennas are preferable options for multiple functions [16-17]. In [17], a miniaturized omnidirectional antenna has two bands, the 403.5 MHz for medical implant communication services (MICS) and the 2.45 GHz for industrial, scientific, and medical (ISM) applications. However, the antenna has complicated structure and increased profile as it consists of two-stacked center-fed circular patch over a circular ground plane. In recent years, the wearable technology has been developed rapidly [18], then, the public is paying more and more attention to the electromagnetic radiation problems of wireless terminals. Under the action of electromagnetic field, the body will produce induction electromagnetic fields as various organs are lossy medium, which lead to electromagnetic energy absorption and dissipation, and then, it is necessary to study the specific absorption rate (SAR) value to evaluate the security performance of the wireless device [19].

The traditional microstrip antennas were widely used because they have many advantages of other antennas, such as low profile, light weight, low cost and easy construction [20]. However, the microstrip antennas have a shortage of narrow bandwidth (typically 2%), and the narrow bandwidth could be a limitation for its applications in WBAN. In order to overcome the shortcoming of narrow bandwidth, bandwidth broadening microstrip antenna technologies had been studied. The most common methods for increasing the bandwidth of the microstrip antenna are shown as follows. The technique of low Q value by low permittivity (air gap), thick substrate and capacitive feeding are used to enhance bandwidth [21], [22]. Multi-layer structure technology and fold structure technology in [23] and [24] lead to high profile and complex structure. Metamaterials in [25] greatly increase the bandwidth of the antenna. In [26], new zeroth-order resonators (ZORs) were utilized as parasitic elements to enhance bandwidth of the microstrip antenna. By utilizing one, two and three resonators, extra corresponding numbers of resonances were generated, by merging the resonances of the resonators with that of the microstrip antenna, the measured impedance bandwidth can be increased from 56 MHz of the reference microstrip antenna to 101, 120, and 133 MHz of the ZORs loaded antennas. However, the parasitic elements lead to antenna size enlargement.

In this article, a novel ZOR-loaded compact microstrip antenna with enhanced bandwidth was proposed for the ISM/MBAN bands and for the brain activity detection in this paper. The wideband performance is achieved by combining the ZOR resonance with the microstrip patch resonance. As the ZOR structure is placed in the interior of the microstrip patch, the antenna size is unchanged with operational frequency decreasing, and the microstrip patch mode still operates good performances. The proposed antenna was measured both in free space and with pork, and reliable off-body performance is achieved. The ZOR antenna has a 150% increasing in the bandwidth compared to the microstrip antenna. In free-space, the simulated and measured -10 dB $|S_{11}|$ bandwidths are 6.7% (2.320-2.481GHz) and 5.5% (2.352-2.487GHz), respectively. As the antenna was mounted as off-body, the simulated and measured impedance bandwidths of the antenna are 5.5% (2.352-2.484 GHz) and 4.7% (2.35-2.465 GHz), respectively. Thus, the antenna meets the MBAN band and the ISM band. The gains at the ZOR mode and microstrip patch mode of the proposed antenna were 2.56 dBi and 4.54 dBi, respectively. In our previous researches for the brain activity detection, antennas were required to radiate face to the head [27-29], and electromagnetic safety would be an issue. Then, (SAR) values of the antenna were calculated by installing the antenna around a human head. Research found that, the antenna radiation meets the health and safety requirements with very small SAR as its backside face the head. While the antenna is installed with its front side face to the brain, 28 mm distance between the brain and the antenna is required.

II. ANTENNA DESIGN AND ANALYSIS

The configurations of the proposed antenna as well as its equivalent circuit were shown in Fig. 1. The proposed antenna consists of two components, a microstrip patch fed by coaxial probe and a ZOR structure embedded in the microstrip patch. The antenna has a substrate dimensions 50mm × 60mm × 1.6mm ($0.384\lambda c \times 0.461\lambda c \times 0.027\lambda c$) and the size of the patch is 28mm × 40mm × 1.6mm ($0.212\lambda c \times 0.310\lambda c \times 0.027\lambda c$). The ZOR's size is only 9mm × 10mm ($0.069\lambda c \times 0.076\lambda c$). Owing to the zero phase constant (β=0) feature of the ZOR, its size can be very small. Then, the ZOR was embedded in the patch, which makes the size and

profile of the proposed antenna is not increased with bandwidth increasing. In this configuration, the bend line acts as a series inductance L_R and the gaps between bend line and the patch generates series capacitance C_L. Since the Q-factor of the resonator is determined by the series inductance and capacitance, the resonant frequency of the ZOR is related to the bending line and the gaps. The proposed antenna was fabricated on a FR4 substrate with a permittivity of 4.4 and thickness of 1.6 mm. The parameters of the antenna are shown below: L_0=50mm, W_0=60, L=28, W=40, a=9, b=10, T=4.5, m=3.3, H_t=2, d=0.6, L_d=0.6, S=4 (unit: mm).

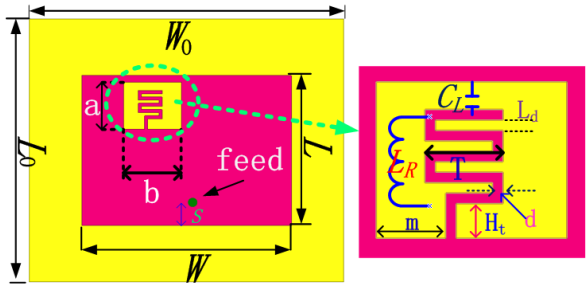

Fig. 1. Configurations of the antenna and its equivalent circuit.

The impedance matching characteristics of the proposed antenna and the reference microstrip antenna (RMA) were compared as shown in Fig. 2. It can be clearly seen that the proposed antenna has an extra ZOR resonance compared to the RMA. Then, the bandwidth of the proposed antenna is increased by 150% compared to the RMA, which completely covers the MBAN and band the ISM band.

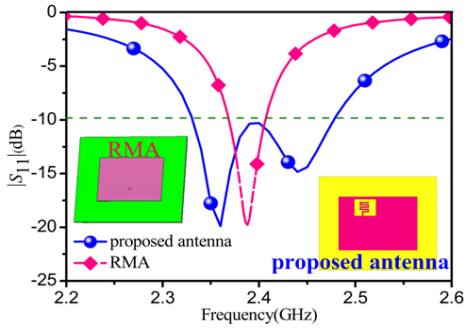

Fig. 2. The simulated $|S_{11}|$ of the proposed antenna and RMA.

ZOR resonances include mu-zero resonator (MZR) and epsilon-zero resonator (EZR) that related to the series and shunt tanks of a composite left and right hand transmission line (CRLH-TL) as shown in Fig. 3 [30-32]. Equations (1) and (2) are the resonant frequencies of the series and shunt tanks, respectively:

$$\omega_{se} = \frac{1}{\sqrt{L_R C_L}}, \tag{1}$$

$$\omega_{sh} = \frac{1}{\sqrt{L_L C_R}}. \tag{2}$$

And the constitutive parameters of the CRLH TL are calculated by Equations (3) and (4):

$$\mu(\omega) = \frac{2Z_B}{j\omega} \bullet \frac{1}{d} = \frac{\left(\frac{\omega}{\omega_{se}}\right)^2 - 1}{\omega^2 C_L} = L_R - \frac{1}{\omega^2 C_L}, \tag{3}$$

$$\varepsilon(\omega) = \frac{Y_B}{j\omega} \bullet \frac{1}{d} = \frac{\left(\frac{\omega}{\omega_{sh}}\right)^2 - 1}{\omega^2 L_L} = C_R - \frac{1}{\omega^2 L_L}. \tag{4}$$

It is found from Equation (3) that the permeability μ is determined by the series tank and it equals zero at the resonance ω_{se}. From the Equation (4), the permittivity ε equals zero at the resonance ω_{sh}. That mean MZR is corresponded to μ = 0, and EZR is related to ε = 0.

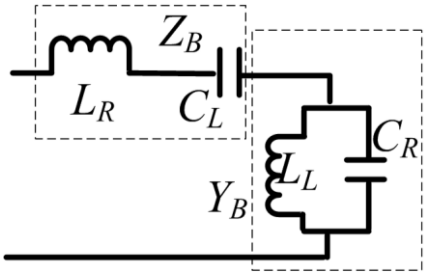

Fig. 3. The equivalent circuit of CRLH-TL.

To verify the ZOR feature of the embedded resonator, the constitutive parameters of the resonator were retrieved by a Kramers-Kroning relationship based metamaterial parameters extraction method [33]. The retrieved method requires the calculation of S parameters. Then, an appropriate simulation model is required to explore the ZOR. As demonstrated in the inset of the Fig. 4, a microstrip line based model was built. A microstrip line has similar field distributions to a microstrip antenna, then, microstrip line based model imitates the operational environment of the ZOR in the microstrip antenna. The microstrip line model used the same substrate as the designed antennas. Figure 4 exhibits the constitutive parameters curves of the ZOR. As shown in the figure, resonance is occurred for the ZOR as large mutations is happened for the effective permittivity (ε_{reff}) and effective permeability (μ_{reff}) curves. For the ZOR, the ε_{reff} is positive in the whole operating band. While the μ_{reff} obtains zero value around 2.35. It can be judged that the embedded structure is a ZOR (MZR) resonator.

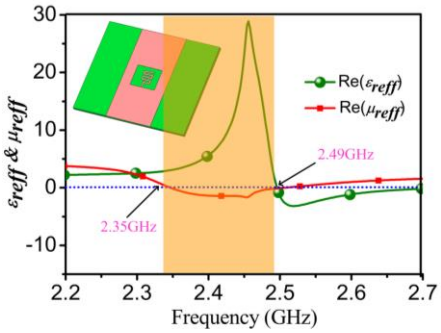

Fig. 4. The simulated dielectric constant and permeability of ZOR structure.

To further reveal the resonances, the impedance curves and the electric field intensity distributions of the proposed antenna were plotted in Fig. 5. From Fig. 5, the antenna has two resonant points. The lower one is the ZOR resonance and the higher one is the microstrip patch resonance. The two resonant points merge with each other wand imply a wide impedance bandwidth. The electric field intensity distributions for the two resonances of the antenna were demonstrated as insets in Fig. 5. At the lower resonance, the electric field is mainly concentrated on the bending line (ZOR structure). At the higher resonance, the electric field is mainly focused on the microstrip patch.

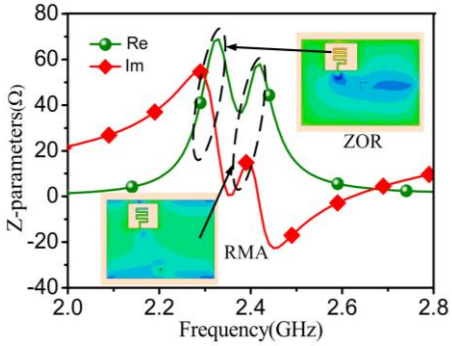

Fig. 5. The electric field intensity distributions and impedance curves of the proposed antenna.

The antenna was fabricated on a 1.6-mm-thick FR4 substrate with a dielectric constant of 4.4 and loss tangent of 0.02. A photograph of the fabricated antenna is shown in Fig. 6 (a). The simulated and measured $|S_{11}|$ of the proposed antenna is shown in Fig. 6 (b). It can be clearly seen that the simulated result is in good agreement with the measured one. Both the measured and simulated -10 dB $|S_{11}|$ bandwidth cover the MBAN band (2.36-2.4 GHz) and the ISM (2.4-2.48 GHz) band completely. In free space, the measured and simulated bandwidths are 133 MHz (2.352-2.485 GHz) and 161 MHz (2.320-2.481 GHz), respectively.

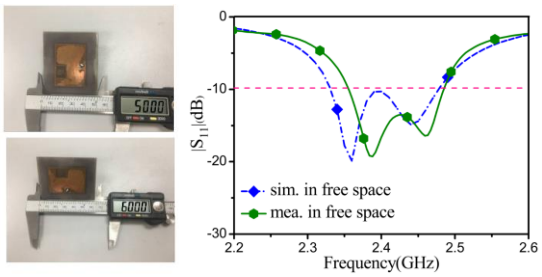

Fig. 6. Photograph of: (a) the fabricated antenna, and (b) the simulated and measured $|S_{11}|$ in free space.

To further investigate the characteristics of the proposed antenna and reveal the independently adjustment of the resonant frequencies, parametric studies were conducted. As shown in Fig. 7, the parameters T and H_t were swept. From Fig. 7 (a), by increasing the parameter T from 4mm to 5.5mm with a step of 0.5mm, the resonance point of ZOR reduce from 2.50 GHz, to 2.35 GHz, 2.25GHz and 2.15 GHz, while microstrip antenna resonant point (MPR) is almost unchanged. Similarly, from Fig. 7 (b), as the height H_t of the ZOR structure increased from 2mm to 3mm with a step of 0.5mm, the ZOR resonant point of the antenna decreased from 2.35 GHz, to 2.30 GHZ and 2.26 GHz, while the MPR was little affected. Thus, it is confirmed that the ZOR resonant point is affected by the parameters of ZOR structure, and the resonant frequencies can be adjusted independently.

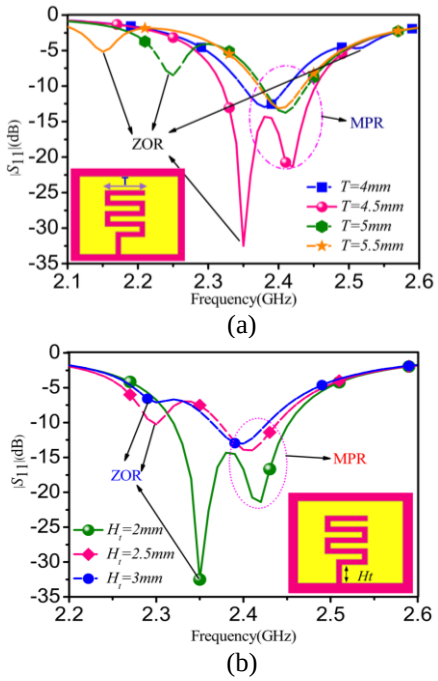

Fig. 7. The simulated $|S_{11}|$ for antenna parameters: (a) T and (b) H_t.

III. ANTENNA OFF-BODY PERFORMANCE

The off-body performances of the antenna was analyzed and compared to the free space performances. In particular, the antenna was simulated under the human equivalent tissue and measured with human arm and pork.

To analyze the off-body performance of the proposed antenna with simulation, the equivalent environment of human tissues should be used. The physical electrical parameters of the human body (tissue) were shown in Table 1 [34-35]. The relative dielectric constant ε_r and loss tangent of human tissue decreased with the frequency increasing. However, the relative conductivity σ increased as the frequency increasing [35]. As the proposed antenna is working at 2.36-2.4 GHz (MABN) and 2.40-2.48 GHz (ISM) bands, the equivalent physical electrical parameters of the tissue in 2.38 GHz and 2.45 GHz were presented in Table 1.

Table 1: Physical electrical parameters of the tissue [34, 35]

Target Frequency (MHz)	Muscle		
	Conductivity [S/m]	Relative Permittivity	Loss Tangent
402-405 (MICS)	0.797	57.106	0.622
600	0.850	55.960	0.455
2360-2400 (MBAN)	1.689	52.820	0.242
2400-2480 (ISM)	1.722	52.760	0.241

In this research, the electrical parameters of the equivalent arm muscles were selected. The equivalent human muscle tissue size is 100mm × 150mm × 50mm. The proposed antenna has a 5mm distance from the tissue to imitate the off-body environment [36]. As the tissue parameters are different for the MBAN and the ISM bands, two equivalent models were established as shown in Fig. 8. In Fig. 8 (a), the equivalent electrical parameters are ε_r=52.820, σ=1.689s/m, tan δ=0.242 for the MBAN band. While in Fig. 7 (b), the physical electrical parameters of the tissue are ε_r=52.760, σ=1.722s/m, tan δ=0.241 for the ISM band.

The results of the simulation and measurement of the fabricated antenna on the free-space and off-body were plotted in Fig. 9. As shown in the figure, in free-space, the simulated and measured $|S_{11}|$ are 2.320-2.481 GHz and 2.352-2.485 GHz, respectively. As the antenna was mounted as off-body, the simulated -10 dB $|S_{11}|$ band is 2.325-2.475 GHz with tissue parameters set at the MBAN band as shown in Fig. 8 (a), while the simulated -10 dB $|S_{11}|$ band for tissue parameters set at the ISM band as shown in Fig. 8 (b) is 2.352-2.484 GHz. Then, both the simulated -10 dB $|S_{11}|$ bands for the tissue parameters settings almost cover the MBAN and the ISM bands. The measured -10 dB $|S_{11}|$ band with the antenna above an arm is 2.35-2.465 GHz. It is found that two resonances were observed for both the free-space and off-body environments.

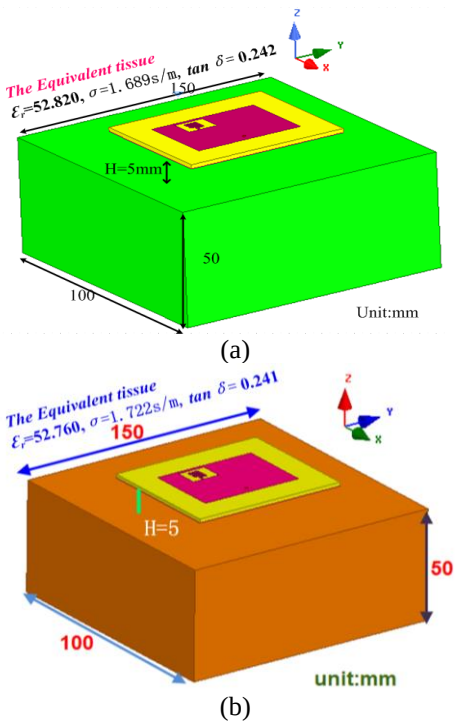

Fig. 8. The model of the proposed antenna and equivalent muscle tissue: (a) at the MABN, and (b) at the ISM.

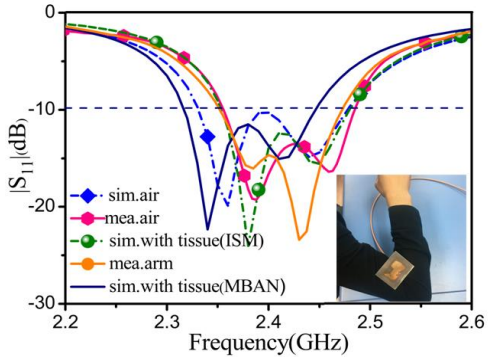

Fig. 9. Simulation and measured $|S_{11}|$ in free-space and the equivalent tissue.

The radiation patterns of the proposed antenna were measured by the NSI2000 system in a microwave anechoic chamber as shown in Fig. 10 (a). Both the patterns in free-space (air) and off-body (pork) were measured [37]. Only half space was measured due to the limitation of the NSI2000 system, and it is enough to verify the simulated results. Radiation patterns of the fabricated antenna were measured at the resonant

frequencies of 2.38 GHz (ZOR) and 2.45 GHz (MPR) as shown in Figs. 10 (b) and (c). The simulated results were also plotted in the figures for comparison. The simulated and measured results show reasonable agreement. As shown in Fig. 10 (b), at 2.38 GHz, the simulated and measured E-plane (xoz-plane φ=0) and H-plane (yoz-plane φ=90°) have good uni-directionally radiation patterns for both the free-space and off-body environments, though the back radiation for off-body environment is larger. At 2.45 GHz, the radiation patterns are similar to 2.38 GHz as shown in Fig. 10 (c). As the size of the ZOR structure is very small, its antenna gain is 2.56 dBi at 2.38 GHz, while the antenna gain for the MPR frequency (2.45 GHz) is 4.54 dBi. In Fig. 10 (d), the antenna efficiency of the RMA is larger than 80%, and the antenna efficiency of the proposed antenna is not bad in the band, such as 70%, though the efficiency drops a few near the ZOR mode. It is clear from Fig. 10 that the proposed antenna maintains good radiation performance both in free-space and off-body. The proposed antenna has relatively stable uni-directional radiation patterns under different environments. The robust off-body performances reveal that the proposed antenna is a good candidate for WBAN applications.

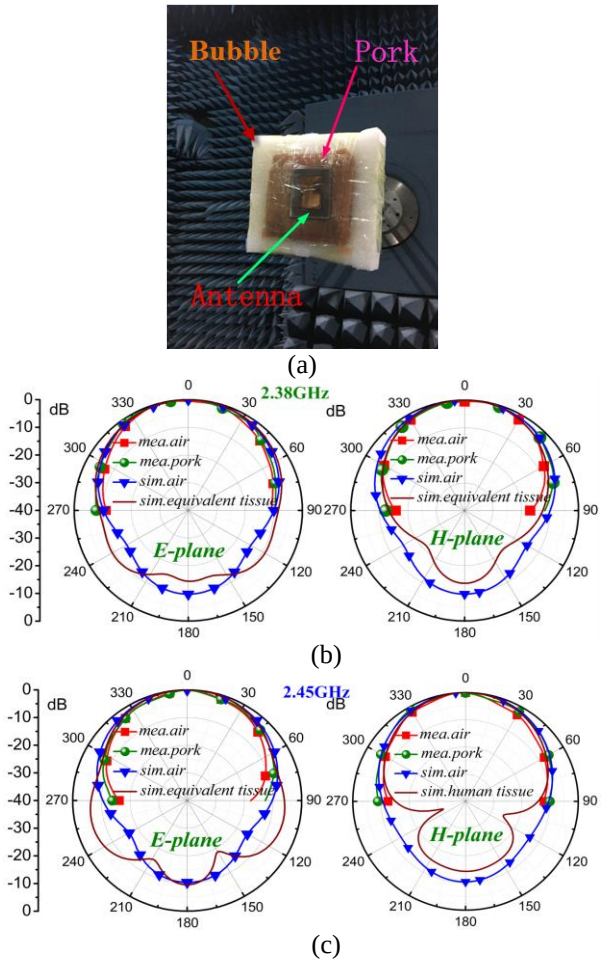

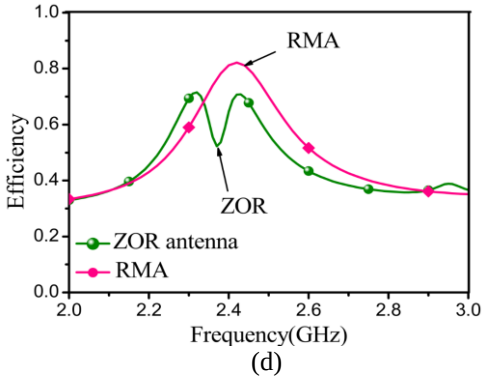

Fig. 10. Simulated/measured radiation patterns in the E-plane and H-plane in free-space and off-body: (a) measurement environment, (b) 2.38 GHz, (c) 2.45 GHz, and (d) efficiencies.

In recent years, there are many studies aiming at abnormal tissue detection such as early breast cancer detection and stroke detection [38, 39] and brain activity detection [27, 28, 29]. For these applications, the SAR level of the antenna needs to be analyzed in the design stage to ensure that the safety limit is obeyed. According to the guidelines of the FCC and the CNIRP, the SAR must not be larger than 2 W/kg averaged over 10g and not greater than 1.6W/kg averaged over 1g of human tissues [40, 41]. The calculated equation for SAR is:

$$SAR = \frac{d}{dt}\left(\frac{dW}{dm}\right) = \frac{d}{dt}\left(\frac{dW}{\rho dV}\right), \quad (5)$$

where W is radiative energy, m is r mass, V is volume and ρ denotes density.

SAR is divided into local SAR and mean SAR. In general, we focus on local SAR, and local SAR values can be obtained by:

$$SAR = \frac{\sigma E}{\rho}, \quad (6)$$

σ is the conductivity, E is the electric field intensity, ρ denotes density.

The input power of 1W is selected as a benchmark to calculate the SAR. The calculation of the SAR and electric field intensity were conducted by the HFSS software. Figures 11 (a) and (b) describe the distribution of electric field intensity for the antenna back size and front size to the antenna, respectively. The SARs with the back size and front size of the antenna to the head were plotted in Figs. 12 (a) and (b), respectively. As shown in Fig. 11 (a) and Fig. 12 (a), when the antenna was back to the brain, the SAR values of the antenna are much smaller than the safety requirement. As shown in Fig. 11 (b), more electromagnetic energy radiates into the brain when the antenna front size to the brain. As shown in Fig. 12 (b), the distance between the antenna and the brain should be larger than 28mm to meet the SAR safety standard.

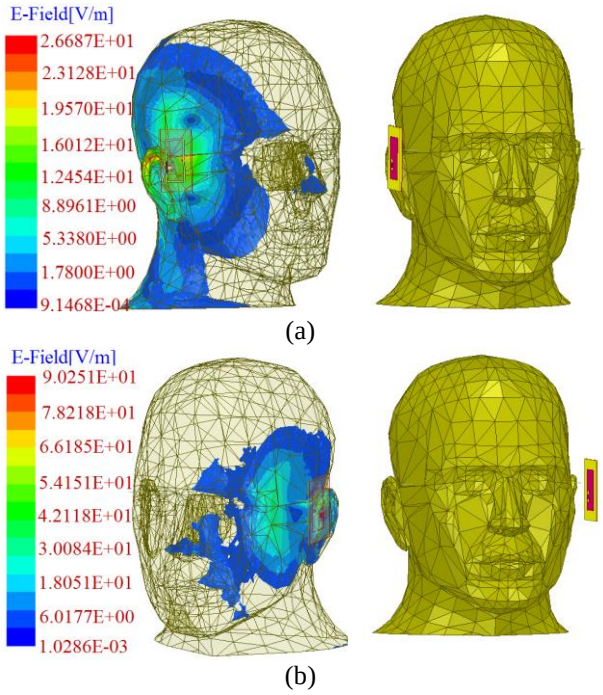

Fig. 11. The distribution of electric field intensities in different situations of the simulation: (a) back and (b) face.

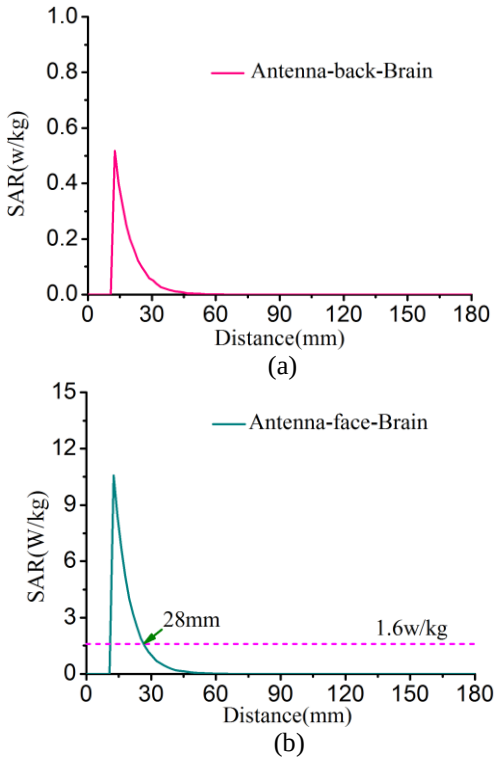

Fig. 12. The antenna of SAR in different situations of the simulation: (a) back and (b) face.

IV. CONCLUSION

In this paper, a novel compact bandwidth enhanced microstrip antenna is designed by loading zeroth-order resonator. The ZOR structure was embedded in the microstrip patch, and the bandwidth of the antenna increased as the adding ZOR resonance. The bandwidth of the antenna increased by 150% compared to the RMA, and it is wide enough to meet the MBAN band and the ISM band. The proposed antenna performances such as reflection characteristic and radiation patterns are examined both in free-space and off-body environments. Robust measured off-body performances were achieved and agree well with the simulation results. The gains of 2.56 dBi and 4.54 dBi were obtained at ZOR frequency and MPR frequency, respectively. The broadband, uni-directional and miniaturization are major advantages that make the proposed antenna can be well applied to WBAN systems. The SAR characteristics of the antenna were also discussed for brain activity detection.

ACKNOWLEDGMENT

This work was supported in part by National Natural Science Foundation of China under Grant Nos. 61661011, 61401110 & 61761012, in part by Natural Science Foundation of Guangxi under Grant No. 2015GXNSFBA139244, in part by Innovation Project of GUET Graduate Education under Grant No. 2017YJCX30, and in part by the project of the basic ability enhancement of Guangxi young teachers under Grant No. 2017KY0204.

REFERENCES

[1] P. S. Hall and Y. Hao, *Antennas and Propagation for Body-Centric Wireless Communications*. Norwood MA, USA: Artech House, 2006. ISBN: 9781608073764.

[2] S. Park and S. Jayaraman, "Enhancing the quality of life through wearable technology," *IEEE Eng. Biol. Mag.*, vol. 22, no. 3, pp. 41-48, 2003.

[3] P. S. Hall, Y. Hao, Y. I. Nechayev, and A. Alomainy, "Antennas and propagation for on-body communication systems," *IEEE Antennas Propag. Mag*., vol. 49, pp. 41-58, 2007.

[4] Y. Peng, X. Wang, L. Guo, Y. Wang, and Q. Deng, "An efficient network coding-based fault-tolerant mechanism in WBAN for smart health-care monitoring systems," *Applied Sciences*, vol. 7, no. 8, pp. 817-835, 2017.

[5] Z. H. Jiang, T. W. Yue, and H. Douglas, *Meta-material-Enabled and Microwave Circuit Integrated Wearable Antennas for Off-body Communications*. in Electromagnetics of Body Area Networks: Antennas, Propagation, and RF Systems, by *Wiley-IEEE Press*, pp. 27-59. 2016.

[6] Federal Communications Commission (FCC): The Medical Implant Communication Services (MICS). Available at: http://wireless.fcc.gov/services/personal/medicalimplant/

[7] IEEE 802.11 Wireless LAN Working Group. Available at: http://www.ieee802.org/11/

[8] FCC, "Federal Communications Commission Revision of Part 15 of the Commission's Rules Regarding Ultra-Wideband Transmission Systems," FCC First Report and Order FCC, April 2002.

[9] Low-Rate Wireless Personal Area Networks (LR-WPANs) Amendment 4, IEEE Standard 802.15.4j-2013.

[10] Y. I. Nechayev, P. S. Hall, and Z. H. Hu, "Characterization of narrowband communication channels on the human body at 2.45 GHz," *IET Microw. Antennas Propag.*, vol. 4, no. 6, pp. 722-732, 2010.

[11] P. J. Soh, G. A. E. Vandenbosch, S. L. Ooi, and N. M. A. Rais, "Design of a broadband all-textile slotted PIFA," *IEEE Trans. Antennas Propag.*, vol. 60, no. 1, pp. 379-384, 2012.

[12] P. J. Soh, G. A. E. Vandenbosch, S. L. Ooi, and M. R. N. Husna, "Wearable dual-band Sierpinski fractal PIFA using conductive fabric," *Electron. Lett.*, vol. 47, no. 6, pp. 365-367, 2011.

[13] A. Alomainy, Y. Hao, A. Owadally, C. G. Parnini, Y. Nechayev, C. C. Constantinou, and P. S. Hall, "Statistical analysis and performance evaluation for on-body radio propagation with microstrip patch antennas," *IEEE Trans. Antennas Propag*., vol. 55, no. 1, pp. 245-248, 2007.

[14] S. Zhu and R. Langley, "Dual-band wearable textile antenna on an EBG substrate," *IEEE Trans. Antennas Propag*., vol. 57, no. 4, pp. 926-935, 2009.

[15] S. Baek and S Lim, "Miniaturised Zeroth-order antenna on spiral slotted ground plane," *Electron. Lett*., vol. 45, no. 20, pp. 1012-1014, 2009.

[16] Z. G. Liu and Y. X. Guo, "Dual band low profile antenna for body centric communications," *IEEE Trans. Antennas. Propag*., vol. 61, no. 4, pp. 2282-2285, 2013.

[17] S. Chamaani and A. Akbarpour, "Miniaturized dual-band omnidirectional antenna for body area network basestations," *IEEE Antennas and Wireless Propagation Letters*, vol. 14, pp. 1722-1725, 2015.

[18] B. W. An, J. H. Shin, S. Y. Kim, J. Kim, S. Ji, J. Park, et al., "Smart sensor systems for wearable electronic devices," *Polymers*, vol. 9, no. 8, pp. 303-344, 2017.

[19] A. Y. I. Ashyap, Z. Z. Abidin, S. H. Dahlan, H. A. Majid, S. M. Shah, M. R. Kamarudin, et al., "Compact and low-profile textile EBG-based antenna for wearable medical applications," *IEEE Antennas & Wireless Propagation Letters*, pp. 99-102, 2017.

[20] A. Sabban, "New wideband printed antennas for medical applications," *IEEE Trans. Antennas Propag*., vol. 61, pp. 84-91, 2013.

[21] A. K. Verma and Nasimuddin, "Resonance frequency of rectangular microstrip antenna on thick substrate," *Electronics Letters*, vol. 37, no. 2, pp. 1373-1374, 2001.

[22] L. Peng, C. L. Ruan, and X. H. Wu, "Design and operation of dual/triple-band asymmetric M-shaped microstrip patch antennas," *IEEE Antennas Wireless Propag. Lett*., vol. 9, no. 1, pp. 1069-1072, 2010.

[23] L. Peng, J. Y. Xie, and S. M. Li, "Wideband microstrip antenna loaded by elliptical rings," *Journal of Electromagn. Waves Appl.*, vol. 30, no. 2, pp. 154-166, 2016.

[24] D. Guha, C. Sarkar, S. Dey, and C. Kuma, "Wide-band high gain antenna realized from simple unloaded single patch," *IEEE Trans. Antennas Propag*., vol. 63, no. 10, pp. 4562-4566, 2015.

[25] Md. Mahmud, M. Islam, N. Misran, M. Singh, K. Mat, "A negative index metamaterial to enhance the performance of miniaturized UWB antenna for microwave imaging applications," *Applied Sciences*, vol. 7, pp. 1149-1165, 2017.

[26] L. Peng, J. Y. Mao, X. F. Li, X. Jiang, and C. L. Ruan, "Bandwidth of microstrip antenna loaded by parasitic zeroth-order resonators," *Microwave and Optical Technology Letters*, vol. 59, no. 5, pp. 1096-1100, 2017.

[27] X. Jiang, B. Kang, X. M. Li, and L. Peng, "Microwave technology for brain activities detection of rats," *International Symposium on Antennas, Propagation and EM Theory IEEE*, pp. 918-920, 2017.

[28] X. Jiang, X. B. Jiang, L. Peng, and X. M. Li, "Microwave transmission approach for human neuronal activities detection," *IEEE International Conference on Microwave and Millimeter Wave Technology IEEE*, pp. 485-487, 2016.

[29] X. Jiang, Z. Geng, X. M. Li, L. Peng, B. Kang, and C. J. Zheng. "Microwave transmission approach for dynamic dielectric detection at brain functional site," *IEEE/mtt-S International Microwave Symposium - IMS IEEE*, pp. 1235-1238, 2017.

[30] A. Lai, K. M. K. H. Leong, and T. Itoh, "Infinite wavelength resonant antennas with monopolar radiation pattern based on periodic structures," *IEEE Trans. Antennas Propag*., pp. 868-876, 2007.

[31] J. H. Park, B. C. Park, Y. H. Ryu, et al., "Modified mu-zero resonator for efficient wireless power transfer," *IET Microwaves, Antennas & Propag.*, no. 8, pp. 912-920, 2014.

[32] L. Peng, J. Y. Xie, X. Jiang, and C. L. Ruan, "Design and analysis of a new ZOR antenna with wide half power beam width (HPBW) characteristic," *Frequenz*, vol. 71, no. 1-2, pp. 41-50, 2017.

[33] Z. Szabo, G. H. Park, R. Hedge, and E. P. Li, "A unique extraction of metamaterial parameters based on Kramers–Kronig relationship," *IEEE Transactions on Microwave Theory and Techniques*, vol. 58, no. 10, pp. 2646-2653, 2010.
[34] K. Chan, R. F. Cleveland, and D. L. Means, "Evaluating compliance with FCC guidelines for human exposure to radiofrequency electromagnetic fields," *Current Reviews in Musculoskeletal Medicine*, vol. 1, no. 2, pp. 88-91, 2001.
[35] IFAC, "Dielectric Properties of Body Tissues," [Online]. Available: http://niremf.ifac.cnr.it/tissprop/htmlclie/htmlclie.php
[36] J. Baek, Y. Lee, and J. Choi, "A wideband Zeroth-order resonance antenna for wireless body area network applications," *IEICE Transactions on Communications*, vol. 10, pp. 2348-235, 2013.
[37] X. Q. Zhu, Y. X. Guo, and W. Wu, "A compact dual-band antenna for wireless body-area network applications," *IEEE Antennas and Wireless Propagation Letters*, vol. 15, pp. 98-101, 2016.
[38] S. Luo, Z. Ji, S. Yang, and D. Xing, "Near-field transmission-type microwave imaging for non-invasive evaluation of electromagnetic characteristics: Towards early breast tumor detection," *IEEE Photonics Journal*, pp. 99, 2017.
[39] Md. D. Hossain and A. S. Mohan, "Cancer detection in highly dense breasts using coherently focused time reversal microwave imaging," *IEEE Trans. on Computational Imaging*, pp. 9, 2017.
[40] A. Ahlbom, U. Bergqvist, J. H. Bernhardt, J. P. Cesarini, M. Grandolfo, M. Hietanen, A. F. Mckinlay, M. H. Repacholi, D. H. Sliney, A. J. Stolwijk, "Guidelines for limiting exposure to time-varying electric, magnetic, and electromagnetic fields (up to 300 GHz)," *International Commission on Non-Ionizing Radiation Protection, Heal. Phys*., vol. 74, pp. 494-522, 1998.
[41] IEEE Recommended Practice for Measurements and Computations of Radio Frequency Electromagnetic Fields with Respect to Human Exposure to Such Fields, 100 kHz–300 GHz, IEEE Std. C95.3-2002, (Revision of IEEE Std. C95.3-1991), pp. i-126.

Kai Sun was born in Zhejiang Province, China, in 1992. He received the B.E. degree in Electronic Information from Hangzhou Dianzi University, Hangzhou, Zhejiang, China, in 2015, and he is currently pursuing a Master's degree in Electronic and Communication Engineering from Guilin University of Electronic Technology (GUET), Guangxi, China. His research interests include antennas and metamaterials.

Lin Peng was born in Guangxi Province, China, in 1981. He received the B.E. degree in Science and Technology of Electronic Information, Master and Doctor's degree in Radio Physics from University of Electronic Science and Technology of China (UESTC), Chengdu, China, in 2005, 2008 and 2013, respectively. From 2011 to 2013, he was sponsored by the China Scholarship Council (CSC) to study at the University of Houston (UH) as joint Ph.D. student. From 2013, he joint Guilin University of Electronic Technology (GUET), and became an Associate Professor from Jan. 2016.

Peng has published over 20 papers as first and corresponding author. He is also co-author with over 20 papers. In recent years, he is sponsored by several funds, such as Fundamental Research Funds for the Central Universities, National Natural Science Foundation of China, Program for Innovative Research Team of Guilin University of Electronic Technology, and Guangxi Wireless Broadband Communication and Signal Processing Key Laboratory, etc. Peng serves as Reviewer for *IEEE TMTT*, *IEEE MWCL*, *IEEE AWPL*, *ACES*, *EL*, *Wireless Personal Communications*, *Progress in Electromagnetics Research*, *IET Microwave, Antennas & Propagation*, and *Journal of Electromagnetic Waves and Applications*.

Peng's research interests include antenna/filter design (for example: communication antennas, Zeroth-Order Resonator (ZOR) antenna, circular-polarized antenna, UWB antenna, microstrip antenna and WLAN antenna), Electromagnetic Bandgap (EBG) structure design and its application in antenna, Composite Right/Left-Handed (CRLH) transmission line and its applications, and conformal antenna array.

Quan Li was born in Shanxi Province, China, in 1991. He received the B.E. degree in Electronic Information College of Electronic Information major of Shaanxi University of Technology, Hanzhong, Shanxi, China, in 2014, and the Master's degree in Electronic and Communication Engineering from Guilin University of Electronic Technology (GUET), Guangxi, China. He is currently a student at the GUET. His research interests include active antenna and dielectric resonant antenna.

Xing Jiang received the Master's degree in Electromagnetic Field and Microwave Technology from Beijing Institute of Technology (BIT), in 1986. From 2000, she joint Guilin University of Electronic Technology (GUET) as Professor. Jiang has published over 30 papers. She also sponsored by National Natural Science Foundation of China and Natural Science Foundation of Guangxi. Jiang is a Senior Member of China Communications Society, a Member of Chinese Institute of Electronics (CIE). Jiang's research interests include smart communication system design, conformal antenna array, and bio-electromagnetics.